Precision Measurement of the Neutron Twist-3 Matrix Element d_2^n: Probing Color Forces

M. Posik,[1,†] D. Flay,[1] D. S. Parno,[2,3] K. Allada,[4] W. Armstrong,[1] T. Averett,[5] F. Benmokhtar,[6,2] W. Bertozzi,[7] A. Camsonne,[8] M. Canan,[9] G. D. Cates,[10] C. Chen,[11] J.-P. Chen,[8] S. Choi,[12] E. Chudakov,[8] F. Cusanno,[13,14] M. M. Dalton,[10] W. Deconinck,[7] C. W. de Jager,[8] X. Deng,[10] A. Deur,[8] C. Dutta,[4] L. El Fassi,[9,15] G. B. Franklin,[2] M. Friend,[2] H. Gao,[16] F. Garibaldi,[13] S. Gilad,[7] R. Gilman,[8,15] O. Glamazdin,[17] S. Golge,[9] J. Gomez,[8] L. Guo,[18] O. Hansen,[8] D. W. Higinbotham,[8] T. Holmstrom,[19] J. Huang,[7] C. Hyde,[9,20] H. F. Ibrahim,[21] X. Jiang,[15,18] G. Jin,[10] J. Katich,[5] A. Kelleher,[5] A. Kolarkar,[4] W. Korsch,[4] G. Kumbartzki,[15] J. J. LeRose,[8] R. Lindgren,[10] N. Liyanage,[10] E. Long,[22] A. Lukhanin,[1] V. Mamyan,[2] D. McNulty,[23] Z.-E. Meziani,[1,‡] R. Michaels,[8] M. Mihovilovič,[24] B. Moffit,[7,8] N. Muangma,[7] S. Nanda,[8] A. Narayan,[25] V. Nelyubin,[10] B. Norum,[10] Nuruzzaman,[25] Y. Oh,[12] J. C. Peng,[26] X. Qian,[16,27] Y. Qiang,[16,8] A. Rakhman,[28] S. Riordan,[10,29] A. Saha,[8,*] B. Sawatzky,[1,8] M. H. Shabestari,[10] A. Shahinyan,[30] S. Širca,[31,24] P. Solvignon,[32,8] R. Subedi,[10] V. Sulkosky,[7,8] W. A. Tobias,[10] W. Troth,[19] D. Wang,[10] Y. Wang,[26] B. Wojtsekhowski,[8] X. Yan,[33] H. Yao,[1,5] Y. Ye,[33] Z. Ye,[11] L. Yuan,[11] X. Zhan,[7] Y. Zhang,[34] Y.-W. Zhang,[34,15] B. Zhao,[5] and X. Zheng[10]

(The Jefferson Lab Hall A Collaboration)

[1]*Temple University, Philadelphia, Pennsylvania 19122, USA*
[2]*Carnegie Mellon University, Pittsburgh, Pennsylvania 15213, USA*
[3]*Center for Experimental Nuclear Physics and Astrophysics, University of Washington, Seattle, Washington 98195, USA*
[4]*University of Kentucky, Lexington, Kentucky 40506, USA*
[5]*College of William and Mary, Williamsburg, Virginia 23187, USA*
[6]*Duquesne University, Pittsburgh, Pennsylvania 15282, USA*
[7]*Massachusetts Institute of Technology, Cambridge, Massachusetts 02139, USA*
[8]*Thomas Jefferson National Accelerator Facility, Newport News, Virginia 23606, USA*
[9]*Old Dominion University, Norfolk, Virginia 23529, USA*
[10]*University of Virginia, Charlottesville, Virginia 22904, USA*
[11]*Hampton University, Hampton, Virginia 23187, USA*
[12]*Seoul National University, Seoul 151-742, South Korea*
[13]*INFN, Sezione di Roma, I-00161 Rome, Italy*
[14]*Istituto Superiore di Sanità, I-00161 Rome, Italy*
[15]*Rutgers, The State University of New Jersey, Piscataway, New Jersey 08855, USA*
[16]*Duke University, Durham, North Carolina 27708, USA*
[17]*Kharkov Institute of Physics and Technology, Kharkov 61108, Ukraine*
[18]*Los Alamos National Laboratory, Los Alamos, New Mexico 87545, USA*
[19]*Longwood University, Farmville, Virginia 23909, USA*
[20]*Université Blaise Pascal/IN2P3, F-63177 Aubière, France*
[21]*Cairo University, Giza 12613, Egypt*
[22]*Kent State University, Kent, Ohio 44242, USA*
[23]*University of Massachusetts, Amherst, Massachusetts 01003, USA*
[24]*Jožef Stefan Institute, SI-1000 Ljubljana, Slovenia*
[25]*Mississippi State University, Mississippi 39762, USA*
[26]*University of Illinois at Urbana-Champaign, Urbana, Illinois 61801, USA*
[27]*Kellogg Radiation Laboratory, California Institute of Technology, Pasadena, California 91125, USA*
[28]*Syracuse University, Syracuse, New York 13244, USA*
[29]*University of Massachusetts, Amherst, Massachusetts 01003, USA*
[30]*Yerevan Physics Institute, Yerevan 375036, Armenia*
[31]*University of Ljubljana, SI-1000 Ljubljana, Slovenia*
[32]*Argonne National Lab, Argonne, Illinois 60439, USA*
[33]*University of Science and Technology of China, Hefei 230026, People's Republic of China*
[34]*Lanzhou University, Lanzhou 730000, Gansu, People's Republic of China*

(Received 15 April 2014; published 11 July 2014)

Double-spin asymmetries and absolute cross sections were measured at large Bjorken x ($0.25 \leq x \leq 0.90$), in both the deep-inelastic and resonance regions, by scattering longitudinally polarized electrons at beam energies of 4.7 and 5.9 GeV from a transversely and longitudinally polarized ^{3}He target. In this dedicated experiment, the spin structure function $g_2^{^3\mathrm{He}}$ was determined with precision at large x, and the neutron twist-3 matrix element d_2^n was measured at $\langle Q^2 \rangle$ of 3.21 and 4.32 GeV$^2/c^2$, with an absolute

 © 2014 American Physical Society

precision of about 10^{-5}. Our results are found to be in agreement with lattice QCD calculations and resolve the disagreement found with previous data at $\langle Q^2 \rangle = 5$ GeV$^2/c^2$. Combining d_2^n and a newly extracted twist-4 matrix element f_2^n, the average neutron color electric and magnetic forces were extracted and found to be of opposite sign and about 30 MeV/fm in magnitude.

DOI: 10.1103/PhysRevLett.113.022002 PACS numbers: 12.38.Aw, 12.38.Qk, 13.88.+e, 14.20.Dh

Over the past 30 years, the availability of polarized targets and lepton beams has enabled an intensive worldwide experimental program of inclusive deep-inelastic scattering (DIS) measurements focused on the investigation of the nucleon spin structure [1]. This led to the confirmation of the Bjorken sum rule [2,3], a fundamental sum rule of quantum chromodynamics (QCD), and the determination of the quarks' spin contribution to the total nucleon spin [1]. Exploration of the nucleon spin structure through QCD has shown that both the g_1 and g_2 spin structure functions of the nucleon contain contributions from the elusive quark-gluon correlations [4–6] beyond the perturbative-QCD radiative corrections [7–9]. In the case of g_1, these correlations emerge at a higher order in the perturbative expansion in powers of the inverse Q^2 (Q^2 is defined as $-q^2$, where q^2 is the virtual photon's four-momentum transfer squared) and thus are suppressed; however, they contribute at leading order in g_2. These correlations manifest themselves in $\bar{g}_2$, a deviation of the measured g_2 from the so-called Wandzura-Wilczek value g_2^{WW} [10] that is expressed solely in terms of the g_1 spin structure function:

$$\bar{g}_2(x, Q^2) = g_2(x, Q^2) - g_2^{\mathrm{WW}}(x, Q^2), \quad (1)$$

$$g_2^{\mathrm{WW}}(x, Q^2) = -g_1(x, Q^2) + \int_x^1 g_1(y, Q^2) dy/y, \quad (2)$$

where x is the Bjorken variable interpreted in the infinite momentum frame as being the fraction of the nucleon's longitudinal momentum carried by the leading struck quark in the DIS process. At present there are no *ab initio* calculations of $\bar{g}_2$. Nevertheless, using the operator product expansion [4,6], the Q^2-dependent quantity

$$d_2 = 3\int_0^1 dx x^2 \bar{g}_2(x) = \int_0^1 dx x^2 [3g_2(x) + 2g_1(x)], \quad (3)$$

can be related to a specific matrix element containing local operators of quark and gluon fields [11,12], and is calculable in lattice QCD [13]. Insight into the physical meaning of d_2 was articulated by Ji [14] who expressed d_2 in terms of a linear combination of χ_E and χ_B, dubbed the electric and magnetic "color polarizabilities," summed over the quark flavors:

$$\chi_E \vec{S} = \frac{1}{2M^2} \langle P, S | q^\dagger \vec{\alpha} \times g\vec{E} q | P, S \rangle, \quad (4)$$

$$\chi_B \vec{S} = \frac{1}{2M^2} \langle P, S | q^\dagger g\vec{B} q | P, S \rangle, \quad (5)$$

where P and S are the nucleon momentum and spin, q and $q^\dagger$ the quark fields, $\vec{E}$ and $\vec{B}$ the average color electric and magnetic fields seen by the struck quark, $\vec{\alpha}$ the velocity of the struck quark, g the strong coupling parameter, and M the nucleon mass.

More recently, Burkardt [15] identified d_2 as being proportional to the instantaneous average sum of the transverse electric F_E and magnetic F_B color forces the struck quark experiences at the instant it is hit by the virtual photon due to the remnant diquark system in the DIS process. The net average force contributes to what is called the "chromodynamic lensing" effect in semi-inclusive DIS where the struck quark experiences color forces as it exits the nucleon before converting into an outbound hadron [15,16]. The relations between the color forces, the color polarizabilities, and the matrix elements of the quark-gluon correlations are given by

$$F_E = -\frac{M^2}{4}\chi_E = -\frac{M^2}{4}\left[\frac{2}{3}(2d_2 + f_2)\right], \quad (6)$$

$$F_B = -\frac{M^2}{2}\chi_B = -\frac{M^2}{2}\left[\frac{1}{3}(4d_2 - f_2)\right], \quad (7)$$

where f_2 is a twist-4 matrix element of the quark-gluon correlation. This twist-4 matrix element cannot be measured directly, but may be extracted by taking advantage of the Q^2 dependence of $g_1(x, Q^2)$ [17,18], since it appears as a higher-order contribution suppressed by $1/Q^2$ in Γ_1, the first moment of g_1.

The neutron d_2 (d_2^n) has been calculated in different nucleon structure models [19–22] and in lattice QCD [13]. The results consistently give a small negative value deviating from the measured positive value by about 2 standard deviations [23,24]. At a fundamental level, the forces d_2 probes are in part responsible for the confinement of the constituents; determining and understanding them in QCD is an important goal. The disagreement between the experimental and theoretical results of d_2^n called for a dedicated measurement.

The E06-014 experiment [25] was performed at Jefferson Lab (JLab) in Hall A [26] from February to March of 2009. In this experiment, measurements of inclusive scattering of a longitudinally polarized electron beam, at an average

current of 15 μA, from a polarized ^{3}He target were carried out at two incident beam energies of 4.7 and 5.9 GeV and with two states of target polarization, transverse (perpendicular to the electron beam in the scattering plane) and longitudinal (along the electron beam). Scattered electrons with momenta ranging from 0.7 to 2 GeV/c were detected in both the BigBite spectrometer (BBS) [27] and the left high-resolution spectrometer (LHRS) [26], each set at a scattering angle of 45°. The large momentum and angular acceptance (~64 msr) of the BBS allowed it to precisely measure the double-spin asymmetries (DSA) over the full momentum range at one current setting of the spectrometer. The absolute cross sections were obtained from the well understood LHRS by scanning over the same momentum range in discrete steps. The longitudinal (transverse) DSA is defined as

$$A_{\parallel(\perp)} = \frac{1}{P_t P_b D_{\mathrm{N}_2}} \frac{1}{\langle \cos\phi \rangle} \frac{N^{\downarrow\Uparrow(\Rightarrow)} - N^{\uparrow\Uparrow(\Rightarrow)}}{N^{\downarrow\Uparrow(\Rightarrow)} + N^{\uparrow\Uparrow(\Rightarrow)}}, \quad (8)$$

where N is the number of detected electrons, P_t is the target polarization, P_b is the electron beam polarization, D_{N_2} is the nitrogen dilution factor that accounts for the small amount (~1% of ^{3}He density) of N_2 present in the ^{3}He target to reduce depolarization effects, and ϕ is the angle between the scattering plane, defined by the initial and final electron momenta, and the polarization plane, defined by the electron and target spins (with $\cos\phi$ applied only to the transverse asymmetry). The single arrows refer to the electron helicity direction and the double arrows refer to the target spin direction. The orientations of the latter are such that arrows pointing to the right (left) represent spins that are transverse to the electron momentum pointing towards the BBS (LHRS), while arrows pointing up (down) represent spins parallel (antiparallel) to the electron momentum.

The incident electron beam polarization was measured using two independent polarimeters based on Møller [28] and Compton [29,30] scattering, whose combined analysis for three run periods yielded electron beam polarizations of $74\% \pm 1\%$ ($E = 5.9$ GeV), $79\% \pm 1\%$ ($E = 5.9$ GeV), and $63\% \pm 1\%$ ($E = 4.7$ GeV) [31]. The residual beam-charge asymmetry was controlled to within 100 ppm through the use of a feedback loop. In a polarized ^{3}He target, the neutron carries the greater part of the nuclear spin, which allows it to serve as an effective neutron target [32]. The scattered electrons interacted with about 10.5 amg (in-beam conditions) of polarized ^{3}He gas contained in a 40-cm-long target cell. The ^{3}He nuclei were polarized via double spin-exchange optical pumping of a Rb-K mixture [33]. Nuclear magnetic resonance (NMR) measurements were taken approximately every 4 hours to monitor the target polarization. The relative NMR measurements were calibrated with absolute electron paramagnetic resonance measurements, which were taken every few days. Additionally, the longitudinal target polarization was cross checked using water NMR measurements. The average target polarization achieved was $50.5\% \pm 3.6\%$ [34].

The BBS consisted of a large-aperture dipole magnet in front of a detector stack whose configuration was similar to that used in Ref. [35] except for the addition of a newly built threshold gas Čerenkov detector [34] used for both electron and positron identification and pion rejection. The magnetic optics software package used for the BBS was calibrated at an incident energy of 1.2 GeV using various targets described in Ref. [35]. Angular and momentum resolutions of 10 mrad and 1% were achieved, respectively [31,34]. To keep trigger rates compatible with a high data-acquisition live time ($\gtrsim$80%), the main electron trigger was formed when signals above threshold were registered in geometrically overlapping regions of the calorimeter and gas Čerenkov. The BBS achieved a total pion rejection factor of better than 10^4.

The LHRS is a small-acceptance spectrometer (~6 msr) and was used with its standard detector package [26]. Optics calibrations [35] for the LHRS used the same targets that were used to calibrate the BBS optics. The LHRS achieved a pion rejection factor of better than 10^5, and measured the e^--^{3}He inclusive cross section to better than 8% (includes statistical and systematic uncertainties added in quadrature).

The two possible sources of background contamination of the electron sample were charged pions and pair-produced electrons resulting from the conversion of π^0 decay photons. The BBS $\pi^-(\pi^+)$ contamination of the $e^-(e^+)$ sample was estimated from the preshower energy spectrum and found to be less than 3% (6.5%) across the momentum acceptance for $\pi^-(\pi^+)$. Weighting the measured $\pi^\pm$ asymmetries by the pion contamination resulted in a negligible pion asymmetry contamination to the electron DSA. The $\pi^\pm$ contamination measured in the LHRS was negligible.

We measured the electron background by assuming it was due to symmetric pair-produced e^+e^- events. Reversing the BBS and LHRS magnet polarities results in positrons rather than electrons being steered into the detectors. By switching the magnet polarity both electrons and positrons should see the same acceptance which then drops out when forming the e^+/e^- ratio. The positron cross section was measured with the LHRS and subtracted from the electron cross section. We used the BBS measured and fitted e^+/e^- ratios, along with statistically weighted positron asymmetry measurements, to determine the amount of pair-production contamination in the electron sample. The e^+/e^- ratio at low x ($\langle x \rangle = 0.277$) was about 56%, and quickly fell off to below 1% ($\langle x \rangle = 0.673$) as x increased. The positron asymmetry was measured with the BBS magnet in normal polarity to be about 1%–2%. The positron asymmetries were cross checked by reversing the BBS magnet polarity and measuring the positron asymmetry for one DSA setting. The background and false asymmetries were removed from the electron asymmetries according to

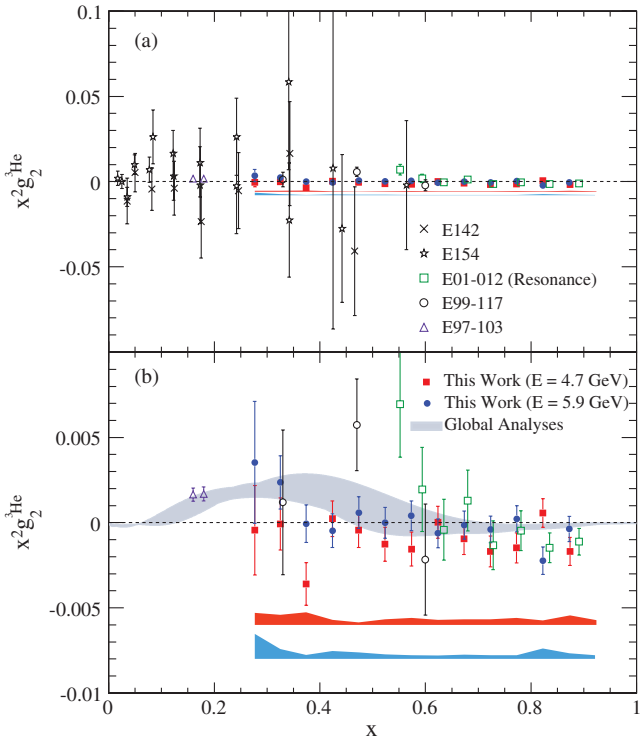


FIG. 1 (color). x^2-weighted $g_2^{^3He}$ plotted against x for data from E99-117 [24], E97-103 [47], E142 [48], E154 [49], and E01-012 [50] with $Q^2 > 1$ GeV$^2/c^2$. (a) All error bars on the world data represent statistical and systematic uncertainties added in quadrature. (b) The error bars on our data are statistical only. The top (red) and bottom (blue) bands represent the systematic uncertainty associated with the $E = 4.7$ and 5.9 GeV data sets, respectively. The gray band shows the $g_2^{WW,^3He}$ coverage from several global analyses [46,51–55].

$$A_{\perp,\parallel}^{e^-} = \frac{A_{\perp,\parallel}^{m,e^-} - c_3 A_{\perp,\parallel}^{m,e^+}}{1 - c_1 - c_3 + c_2 c_3}, \tag{9}$$

where c_1 is the π^-/e^- ratio, c_2 is the π^+/e^+ ratio, c_3 is the e^+/e^- ratio, and $A_{\perp,\parallel}^{m,e^-(e^+)}$ is the measured electron (positron) asymmetry.

Lastly, the electromagnetic internal and external radiative corrections were performed on the unpolarized cross section σ_0 using the formalism of Mo and Tsai [36,37]. The elastic [36] and quasielastic [38] radiative tails were subtracted using form factors from Refs. [39,40]. The inelastic corrections were evaluated using the F1F209 parametrization [41] for the unmeasured cross sections in the resonance and DIS regions. We followed the formalism of Akushevich *et al.* [42] to perform the radiative corrections on $\Delta\sigma_{\parallel,\perp} = 2\sigma_0 A_{\parallel,\perp}$, the polarized cross-section differences. Here, the tails from the polarized elastic cross-section differences were found to be negligible. The remaining quasielastic [43,44], resonance [45], and deep-inelastic regions [46] were treated together using inputs from their respective models. The size of the total correction in all cases did not exceed 45% of the measured σ_0, $\Delta\sigma_\parallel$, and $\Delta\sigma_\perp$. Although the magnitude of this correction is significant, the associated absolute uncertainty on the radiative corrections on g_1 and g_2 was less than 5%, which is smaller than their statistical uncertainty.

In Fig. 1 we show the x^2-weighted polarized spin structure function g_2 of ^{3}He, formed from the measured Born asymmetries and cross sections according to

$$g_2^{^3He} = \frac{MQ^2}{4\alpha^2}\frac{y^2\sigma_0}{(1-y)(2-y)} \times \left[-A_\parallel^{e^-} + \frac{1+(1-y)\cos\theta}{(1-y)\sin\theta}A_\perp^{e^-}\right], \tag{10}$$

where α is the electromagnetic coupling constant, $y = (E - E')/E$ is the fraction of the incident electron energy loss in the nucleon rest frame, E is the incident electron energy, E' is the scattered electron energy, and θ is the electron scattering angle. Note the dramatic improvement of the statistical precision of our data in Fig. 1(a) compared to the available ^{3}He world data; Fig. 1(b) is zoomed in by a factor of 10 and shows only a subset of the world data.

The measured DSAs and cross sections at each beam energy were used to evaluate $d_2^{^3He}$ at two $\langle Q^2\rangle$ values (3.21 and 4.32 GeV$^2/c^2$) according to

$$d_2^{^3He} = \int_{0.25}^{0.90} dx \frac{MQ^2}{4\alpha^2}\frac{x^2y^2\sigma_0}{(1-y)(2-y)} \times \left[\left(3\frac{1+(1-y)\cos\theta}{(1-y)\sin\theta} + \frac{4}{y}\tan\frac{\theta}{2}\right)A_\perp^{e^-} + \left(\frac{4}{y} - 3\right)A_\parallel^{e^-}\right]. \tag{11}$$

The upper integration limit of $x = 0.90$ was chosen in order to avoid the quasielastic peak and the Δ resonance. In addition to using Eq. (11), the Nachtmann moments [56] may be used to evaluate $d_2^{^3He}$, but the difference between the two approaches at our kinematics is smaller than the statistical precision of our measured $d_2^{^3He}$ value. Neutron information was extracted from $d_2^{^3He}$ through the expression

TABLE I. Measured values of d_2^n.

$\langle Q^2\rangle$ (GeV$^2/c^2$)	Measured ($\times 10^{-5}$)	Low x ($\times 10^{-5}$)	Elastic ($\times 10^{-5}$)	Total d_2^n ($\times 10^{-5}$)
3.21	$-261.0 \pm 79.0_{\text{stat}} \pm 48.0_{\text{sys}}$	$38.0 \pm 58.0_{\text{sys}}$	$-198.0 \pm 32.0_{\text{sys}}$	$-421.0 \pm 79.0_{\text{stat}} \pm 82.0_{\text{sys}}$
4.32	$4.0 \pm 83.0_{\text{stat}} \pm 37.0_{\text{sys}}$	$38.0 \pm 58.0_{\text{sys}}$	$-77.0 \pm 9.0_{\text{sys}}$	$-35.0 \pm 83.0_{\text{stat}} \pm 69.0_{\text{sys}}$

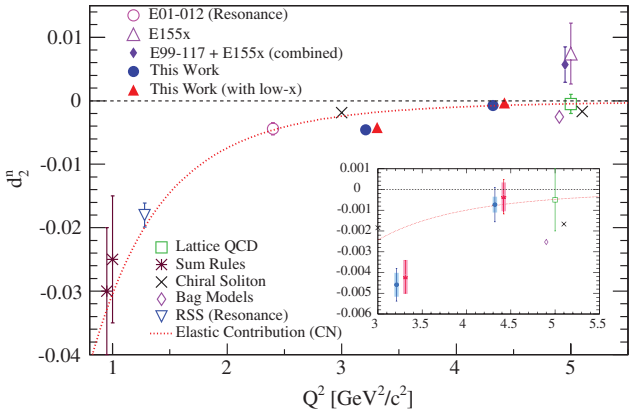


FIG. 2 (color). d_2^n data plotted against Q^2 for data with $\langle Q^2 \rangle \geq 1$ GeV$^2/c^2$. The error bars on the world data from E01-012 [50], E155x [23], E99-117 + E155x [24], and RSS [62] represent the in quadrature sum of their statistical and systematic uncertainties. Our results are displayed with and without the low-x contribution added, and are offset in Q^2 for clarity. The inset figure zooms in around our results, with the shaded boxes representing our systematic uncertainty.

$$d_2^n = \frac{d_2^{^3\mathrm{He}} - (2P_p - 0.014)d_2^p}{P_n + 0.056}, \tag{12}$$

where P_p and P_n are the effective proton and neutron polarizations in ^{3}He, and the factors 0.056 and 0.014 are due to the Δ-isobar contributions [32]. d_2^p in Eq. (12) was calculated from various global analyses [46,51–55] to be $(-17.5 \pm 5.3) \times 10^{-4}$ and $(-16.9 \pm 4.7) \times 10^{-4}$ at the kinematics of E06-014 at average $\langle Q^2 \rangle$ values of 3.21 (where Q^2 ranged from about 2.0 to 4.9 GeV$^2/c^2$) and 4.32 GeV$^2/c^2$ (where Q^2 ranged from about 2.6 to 6.6 GeV$^2/c^2$), respectively. Additionally, other neutron extraction methods were studied in Ref. [57]; those results were found to be consistent within our total uncertainty.

The d_2^n values measured during E06-014 represent only partial integrals. The full integrals can be evaluated by computing the low- and high-x contributions. The low-x contribution is suppressed due to the x^2 weighting of the d_2 integrand, and was calculated by fitting existing g_1^n [47–49,58] and g_2^n [23,47,59] data. The fits to both structure functions were dominated by the precision data from Ref. [47], and extended in x from 0.02 to 0.25. A possible Q^2 dependence of this low-x contribution was presumed to be negligible in this analysis. The high-x contribution, dominated by the elastic $x = 1$ contribution with a negligible contribution from $0.9 < x < 1$, was estimated using the elastic form factors G_E^n and G_M^n, computed from the parametrizations given in Refs. [60,61], respectively. The individual contributions used to evaluate the full d_2^n integral are listed in Table I.

The fully integrated d_2^n results from this experiment are shown as a function of Q^2 in Fig. 2 along with the world data and available calculations. Our d_2^n results are in agreement with the lattice QCD [13] (evaluated at $Q^2 = 5$ GeV$^2/c^2$), bag model [21] (evaluated at $Q^2 = 5$ GeV$^2/c^2$), and chiral soliton model [22] (evaluated at $Q^2 = 3$ and 5 GeV$^2/c^2$) calculations, which predict a small negative value of d_2^n at large Q^2. We note that at lower Q^2, the elastic contribution of d_2^n dominates the measured values and is in agreement with the QCD sum rule calculations [19,20] (evaluated at $Q^2 = 1$ GeV$^2/c^2$). Given our precision, we find a d_2^n value near $Q^2 = 5$ GeV^2 that is about 3 standard deviations smaller than the lowest error bar reported by SLAC E155x.

Primed with a new value of d_2^n, we proceeded to determine f_2^n and extract the average electric and magnetic color forces. The quantity f_2^n was extracted following the analysis described in Refs. [17,34]. Our f_2^n extraction used a_2^n matrix elements evaluated from global analyses [46,51–55], which were found to be $(4.3 \pm 12.1) \times 10^{-4}$ and $(0.6 \pm 11.3) \times 10^{-4}$ at $\langle Q^2 \rangle = 3.21$ and 4.32 GeV$^2/c^2$, respectively, our measured d_2^n values, and the inclusion of the Γ_1 data from the JLab RSS experiment [62] and the most recent JLab E94-010 data [63]. The singlet axial charge $\Delta\Sigma$ was determined from values of Γ_1^n at $Q^2 \geq 5$ GeV$^2/c^2$ to be 0.375 ± 0.052, in excellent agreement with that found in Ref. [64]. We note that our extracted f_2^n values are consistent with the value found in Ref. [17]. A summary of our f_2^n and average color force values, along with calculations from several models, are presented in Table II.

In summary, we have measured the DSA and unpolarized cross sections from a polarized ^{3}He target, allowing for the precision measurement of the neutron d_2. We find that d_2^n is small and negative at $\langle Q^2 \rangle = 3.21$ and 4.32 GeV$^2/c^2$. We find that our results are consistent with the lattice QCD [13], bag model [21], and chiral soliton [22] predictions.

TABLE II. Our results for f_2^n, F_E^n, and F_B^n compared to model calculations. The value for d_2^n is assumed to be zero in the instanton model calculation, as it is much smaller than f_2^n [65]. Note that we have divided Eqs. (6) and (7) by $\hbar c$ to obtain force units of MeV/fm.

Group	Q^2(GeV$^2/c^2$)	$f_2^n \times 10^{-3}$	F_E^n (MeV/fm)	F_B^n (MeV/fm)
E06-014	3.21	$43.57 \pm 0.79_{\mathrm{stat}} \pm 39.38_{\mathrm{sys}}$	$-26.17 \pm 1.32_{\mathrm{stat}} \pm 29.35_{\mathrm{sys}}$	$44.99 \pm 2.43_{\mathrm{stat}} \pm 29.43_{\mathrm{sys}}$
E06-014	4.32	$39.80 \pm 0.83_{\mathrm{stat}} \pm 39.38_{\mathrm{sys}}$	$-29.12 \pm 1.38_{\mathrm{stat}} \pm 29.34_{\mathrm{sys}}$	$30.68 \pm 2.55_{\mathrm{stat}} \pm 29.40_{\mathrm{sys}}$
Instanton [65,66]	0.40	38.0	−30.41	30.41
QCD sum rule [12,19]	1	-13.0 ± 6.0	54.25 ± 15.52	79.52 ± 30.06
QCD sum rule [20]	1	10.0 ± 10.0	29.73 ± 16.62	81.75 ± 30.64

We used our d_2^n measurements to extract the twist-4 matrix element f_2^n and performed a decomposition into neutron average electric and magnetic color forces. We note that our extracted f_2^n is larger than our measured d_2^n, implying that the neutron electric and magnetic color forces are nearly equal in magnitude but opposite in sign.

We would like to thank the JLab Hall A technical staff and Accelerator Division for their outstanding support, as well as M. Burkardt, L. P. Gamberg, W. Melnitchouk, A. Metz, and J. Soffer for their useful discussions. One of us (Z.-E. M.) would like to particularly thank X.-D. Ji for his encouragement to propose and perform this measurement since 1995. This work was supported in part by DOE Grants No. DE-FG02-87ER40315 and No. DE-FG02-94ER40844 (from Temple University). Jefferson Lab is operated by the Jefferson Science Associates, LLC, under DOE Grant No. DE-AC05-060R23177.

*Deceased.
†posik@temple.edu
‡meziani@temple.edu

[1] C. A. Aidala, S. D. Bass, D. Hasch, and G. K. Mallot, Rev. Mod. Phys. **85**, 655 (2013), and references therein.
[2] J. D. Bjorken, Phys. Rev. **148**, 1467 (1966).
[3] J. D. Bjorken, Phys. Rev. D **1**, 1376 (1970).
[4] E. V. Shuryak and A. I. Vainshtein, Nucl. Phys. **B201**, 141 (1982).
[5] R. L. Jaffe, Comments Nucl. Part. Phys. **19**, 239 (1990).
[6] R. L. Jaffe and X.-D. Ji, Phys. Rev. D **43**, 724 (1991).
[7] V. N. Gribov and L. N. Lipatov, Yad. Fiz. **15**, 781 (1972) [Sov. J. Nucl. Phys. **15**, 438 (1972)].
[8] G. Altarelli and G. Parisi, Nucl. Phys. **B126**, 298 (1977).
[9] Yu. L. Dokshitzer, Sov. Phys. JETP **46**, 641 (1977).
[10] S. Wandzura and F. Wilczek, Phys. Lett. **72B**, 195 (1977).
[11] X.-D. Ji and P. Unrau, Phys. Lett. B **333**, 228 (1994).
[12] E. Stein, P. Gornicki, L. Mankiewicz, and A. Schafer, Phys. Lett. B **353**, 107 (1995).
[13] M. Göckeler, R. Horsley, D. Pleiter, P. Rakow, A. Schäfer, G. Schierholz, H. Stüben, and J. Zanotti, Phys. Rev. D **72**, 054507 (2005).
[14] X.-D. Ji, in *Proceedings of the 7th International Conference on the Structure of Baryons, Santa Fe, 1995*, edited by P. D. Barnes and J. B. McClelland (World Scientific, Singapore, 1996) pp. 25–34; arXiv:hep-ph/9510362.
[15] M. Burkardt, Phys. Rev. D **88**, 114502 (2013).
[16] M. Burkardt, Nucl. Phys. **A735**, 185 (2004).
[17] Z.-E. Meziani *et al.*, Phys. Lett. B **613**, 148 (2005).
[18] M. Osipenko, W. Melnitchouk, S. Simula, P. Bosted, V. Burkert, M. E. Christy, K. Griffioen, C. Keppel, and S. E. Kuhn, Phys. Lett. B **609**, 259 (2005).
[19] E. Stein, P. Gornicki, L. Mankiewicz, A. Schafer, and W. Greiner, Phys. Lett. B **343**, 369 (1995).
[20] I. I. Balitsky, V. M. Braun, and A. V. Kolesnichenko, Phys. Lett. B **242**, 245 (1990); **318**, 648(E) (1993).
[21] X. Song, Phys. Rev. D **54**, 1955 (1996).
[22] H. Weigel, L. P. Gamberg, and H. Reinhardt, Phys. Rev. D **55**, 6910 (1997).
[23] P. L. Anthony *et al.* (E155 Collaboration), Phys. Lett. B **553**, 18 (2003).
[24] X. Zheng *et al.* (Jefferson Lab Hall A Collaboration), Phys. Rev. C **70**, 065207 (2004).
[25] S. Choi, X. Jiang, Z.-E. Meziani, B. Sawatzky, Spokespersons, Jefferson Lab Experiment E06-014, http://www.jlab.org/exp_prog/proposals/06/PR06-014.pdf.
[26] J. Alcorn *et al.*, Nucl. Instrum. Methods Phys. Res., Sect. A **522**, 294 (2004).
[27] D. J. J. de Lange, J. J. M. Steijger, H. de Vries, M. Anghinolfi, M. Taiuti, D. W. Higinbotham, B. E. Norum, and E. Konstantinov, Nucl. Instrum. Methods Phys. Res., Sect. A **406**, 182 (1998).
[28] A. V. Glamazdin *et al.*, Fiz. B **8**, 91 (1999).
[29] S. Escoffier *et al.*, Nucl. Instrum. Methods Phys. Res., Sect. A **551**, 563 (2005).
[30] M. Friend *et al.*, Nucl. Instrum. Methods Phys. Res., Sect. A **676**, 96 (2012).
[31] D. Parno, Ph. D. thesis, Carnegie Mellon University (unpublished).
[32] F. R. P. Bissey, V. A. Guzey, M. Strikman, and A. W. Thomas, Phys. Rev. C **65**, 064317 (2002).
[33] E. Babcock, I. Nelson, S. Kadlecek, B. Driehuys, L. Anderson, F. Hersman, and T. Walker, Phys. Rev. Lett. **91**, 123003 (2003).
[34] M. Posik, Ph. D. thesis, Temple University (unpublished).
[35] X. Qian *et al.* (Jefferson Lab Hall A Collaboration), Phys. Rev. Lett. **107**, 072003 (2011).
[36] L. W. Mo and Y.-S. Tsai, Rev. Mod. Phys. **41**, 205 (1969).
[37] Y.-S. Tsai, Report No. SLAC-PUB-0848.
[38] S. Stein, W. Atwood, E. Bloom, R. Cottrell, H. DeStaebler, C. Jordan, H. Piel, C. Prescott, R. Siemann, and R. Taylor, Phys. Rev. D **12**, 1884 (1975).
[39] A. Amroun *et al.*, Nucl. Phys. **A579**, 596 (1994).
[40] J. W. Lightbody and J. S. O'Connell, Comput. Phys. **2**, 57 (1988).
[41] P. E. Bosted and V. Mamyan, arXiv:1203.2262.
[42] I. Akushevich, A. Ilyichev, N. Shumeiko, A. Soroko, and A. Tolkachev, Comput. Phys. Commun. **104**, 201 (1997).
[43] P. E. Bosted, Phys. Rev. C **51**, 409 (1995).
[44] J. Amaro, M. Barbaro, J. Caballero, T. Donnelly, A. Molinari, and I. Sick, Phys. Rev. C **71**, 015501 (2005).
[45] D. Drechsel, S. S. Kamalov, and L. Tiator, Eur. Phys. J. A **34**, 69 (2007).
[46] D. de Florian, R. Sassot, M. Stratmann, and W. Vogelsang, Phys. Rev. Lett. **101**, 072001 (2008).
[47] K. Kramer *et al.*, Phys. Rev. Lett. **95**, 142002 (2005).
[48] P. L. Anthony *et al.* (E142 Collaboration), Phys. Rev. D **54**, 6620 (1996).
[49] K. Abe *et al.* (E154 Collaboration), Phys. Lett. B **404**, 377 (1997).
[50] P. Solvignon *et al.* (E01-012 Collaboration), arXiv:1304.4497.
[51] D. de Florian, G. A. Navarro, and R. Sassot, Phys. Rev. D **71**, 094018 (2005).
[52] C. Bourrely, J. Soffer, and F. Buccella, Eur. Phys. J. C **23**, 487 (2002).
[53] C. Bourrely, J. Soffer, and F. Buccella, Phys. Lett. B **648**, 39 (2007).

[54] E. Leader, A. V. Sidorov, and D. B. Stamenov, Phys. Rev. D **73**, 034023 (2006).
[55] T. Gehrmann and W. J. Stirling, Phys. Rev. D **53**, 6100 (1996).
[56] O. Nachtmann, Nucl. Phys. **B63**, 237 (1973).
[57] J. J. Ethier and W. Melnitchouk, Phys. Rev. C **88**, 054001 (2013).
[58] K. Abe *et al.* (E143 Collaboration), Phys. Rev. D **58**, 112003 (1998).
[59] P. L. Anthony *et al.* (E155 Collaboration), Phys. Lett. B **458**, 529 (1999).
[60] S. Riordan *et al.*, Phys. Rev. Lett. **105**, 262302 (2010).
[61] J. J. Kelly, Phys. Rev. C **70**, 068202 (2004).
[62] K. Slifer *et al.* (RSS Collaboration), Phys. Rev. Lett. **105**, 101601 (2010).
[63] K. Slifer *et al.* (E94010 Collaboration), Phys. Rev. Lett. **101**, 022303 (2008).
[64] A. Accardi *et al.*, arXiv:1212.1701.
[65] J. Balla, M. V. Polyakov, and C. Weiss, Nucl. Phys. **B510**, 327 (1998).
[66] N.-Y. Lee, K. Goeke, and C. Weiss, Phys. Rev. D **65**, 054008 (2002).